Available online at www.sciencedirect.com
SCIENCE DIRECT
Journal of Petroleum Science and Engineering 51 (2006) 253–266
JOURNAL OF PETROLEUM SCIENCE & ENGINEERING
www.elsevier.com/locate/petrol

Prediction of thermodynamic properties of natural gas mixtures using 10 equations of state including a new cubic two-constant equation of state

Kh. Nasrifar *, O. Bolland

Department of Energy and Process Engineering, Norwegian University of Science and Technology (NTNU), NO-7491 Trondheim, Norway

Received 27 April 2005; received in revised form 29 September 2005; accepted 14 January 2006

Abstract

In this contribution, 10 equations of state (EoSs) are used to predict the thermo-physical properties of natural gas mixtures. One of the EoSs is proposed in this work. This EoS is obtained by matching the critical fugacity coefficient of the EoS to the critical fugacity coefficient of methane. Special attention is given to the supercritical behavior of methane as it is the major component of natural gas mixtures and almost always supercritical at reservoir and surface conditions. As a result, the proposed EoS accurately predicts the supercritical fugacity of methane for wide ranges of temperature and pressure. Using the van der Waals mixing rules with zero binary interaction parameters, the proposed EoS predicts the compressibility factors and speeds of sound data of natural gas mixtures with best accuracy among the other EoSs. The average absolute error was found to be 0.47% for predicting the compressibility factors and 0.70% for the speeds of sound data. The proposed EoS was also used to predict thermal and equilibrium properties. For predicting isobaric heat capacity, Joule–Thomson coefficient, dew points and flash yields of natural gas mixtures, the predictive accuracy of the EoS is comparable to the predictive accuracy of the Redlich–Kwong–Soave (RKS) EoS or one of its variants. For predicting saturated liquid density of LNG mixtures, however, the accuracy of predictions is between the RKS and Peng–Robinson (PR) EoSs.

Keywords: Natural gas; Thermodynamic property; Compressibility factor; Speeds of sound; Phase equilibrium; Equation of state

1. Introduction

Predicting the thermodynamic properties of natural gas mixtures are important in gas industry—that is in production, processing, storage and transportation. Accurate values of natural gas compressibility factors and speeds of sound data are crucial in custody transfer operations. Other thermodynamic properties, e.g., saturated liquid density of liquefied natural gas (LNG) mixtures, are used in the design of liquefaction processes and storage facilities; Joule–Thomson coefficients are used in throttling processes and dew points are used in pipeline design.

There are accurate correlations/equations of state (EoSs) for calculating natural gas properties. McCarty (1982) reported an accurate extended corresponding states (ECS) model for LNG systems. Using ECS models, Estela-Uribe and Trusler (2001) and Estela-Uribe et al. (2004) predicted the compressibility factors,

* Corresponding author. Tel.: +47 735 98462; fax: +47 735 98390.
E-mail address: khashayar.nasrifar@ntnu.no (Kh. Nasrifar).

0920-4105/$ - see front matter © 2006 Elsevier B.V. All rights reserved.
doi:10.1016/j.petrol.2006.01.004

densities, speeds of sound and bubble point pressures of natural gas mixtures quite accurately. Accurate models, for instance, AGA NX-19 (1978) and MGERG-88 (Jaeschke et al., 1989) are used in custody transfer for calculating compressibility factors of natural gas mixtures. The Benedict et al. (1940) (BWR) EoS, modified Redlich and Kwong (1949) (RK) EoS by Soave (1972) (RKS) and Peng and Robinson (1976) (PR) EoS are often used in the gas industry for predicting natural gas equilibrium properties.

Except the RKS and PR EoSs, the other models are either complex or require many pure component constants and/or binary parameters (Estela-Uribe et al., 2004). For instance, the BWR EoS has 8 constants. The MGERG (Jaeschke et al., 1989) model is not suitable for thermal properties calculations. The ECS models of Estela-Uribe and Trusler (2001) and Estela-Uribe et al. (2004) take the advantage of binary parameters, and therefore cannot be extended to natural gas mixtures with heavy fractions.

The RKS and PR EoSs are often used in the gas industry as predictive tools. When these two EoSs are compared with the mentioned models above, they are rather accurate. Moreover, both EoSs take the advantage of simplicity. They are reliable and predict the thermodynamic properties of natural gas mixtures with reasonable accuracy. In addition, these two EoSs can be used for predicting the properties of natural gas mixtures containing heavy fractions (Nasrifar et al., 2005).

Natural gas mixtures comprise supercritical methane as the major component. When the new findings in supercritical behavior of EoSs are taken into account (Mathias, 2003); an accurate EoS can be constructed for application in the gas industry. The objective of this work is to obtain a predictive two-constant EoS. This EoS should exhibit an accurate description of thermodynamic properties of natural gas mixtures while preserving the outstanding characteristics of the RKS and PR equations.

2. Model development

Natural gas mixtures comprise of many hydrocarbon and non-hydrocarbon constituents with methane as the major component. Heavy hydrocarbons up to C_{40} sometimes exist in natural gas mixtures. Nitrogen, carbon dioxide and hydrogen sulfide are usually the non-hydrocarbon components. While the gas phase properties of natural gas mixtures, to a large extent, result from the presence of methane, the equilibrium properties are affected by the presence of heavier hydrocarbons (Nasrifar et al., 2005). Thus, the EoS of natural gas mixtures must be accurate at representing methane and heavier hydrocarbon properties as limiting cases of the mixture true behavior. However, this is only a necessary condition.

The pressure and temperature of most natural gas mixtures, at reservoir and surface conditions, can be found up to 150 MPa and 500 K, respectively. At these conditions, nitrogen, methane and ethane are almost always supercritical while the heavier hydrocarbons are subcritical. In other words, to accurately describe the properties of natural gas mixtures, the supercritical behavior of methane and to a less extent nitrogen and ethane, and the subcritical behavior of heavy hydrocarbons should be accurately described. In an EoS, the

Table 1
Accuracy (%AAD) of the EoSs in predicting the vapor pressure of some natural gas constituents (experimental data from Daubert and Danner, 1992)

Component	T_r range	This work	RKS/RKSNB	RKTCC	PR	PRGGPR	MNM	3M
H_2S	0.50–1	3.04	2.30	3.75	3.91	3.42	3.75	3.52
CO_2	0.71–1	0.99	0.44	0.11	0.52	0.14	1.27	2.67
C_1	0.48–1	1.66	2.02	0.26	0.50	1.06	0.79	3.14
C_2	0.30–1	2.28	3.60	1.83	3.46	1.45	7.26	3.54
C_3	0.23–1	2.33	3.08	7.37	9.37	3.53	13.72	4.06
i-C_4	0.29–1	8.55	7.17	4.40	16.33	9.09	3.40	8.86
n-C_4	0.32–1	1.80	2.30	3.00	4.33	0.85	5.85	6.49
i-C_5	0.25–1	2.33	2.50	7.78	11.81	1.25	12.73	7.89
n-C_5	0.30–1	6.76	6.04	2.35	14.79	8.39	4.26	10.40
n-C_6	0.35–1	4.80	4.88	2.32	8.44	5.03	2.47	11.73
n-C_8	0.38–1	2.51	2.11	3.50	3.53	1.79	5.02	11.93
n-C_{12}	0.40–1	2.08	1.69	2.34	9.00	3.65	4.13	16.34
n-C_{16}	0.40–1	4.36	3.54	4.00	11.73	2.18	8.36	18.48
n-C_{20}	0.40–1	3.26	4.03	4.35	25.90	7.04	9.89	26.22
C_6H_6	0.49–1	1.63	0.78	1.11	1.59	1.67	1.27	5.05
cyc-C_5	0.35–1	1.79	1.15	0.87	5.10	2.67	2.60	4.69
Average		3.14	2.98	3.08	8.14	3.33	5.42	9.06

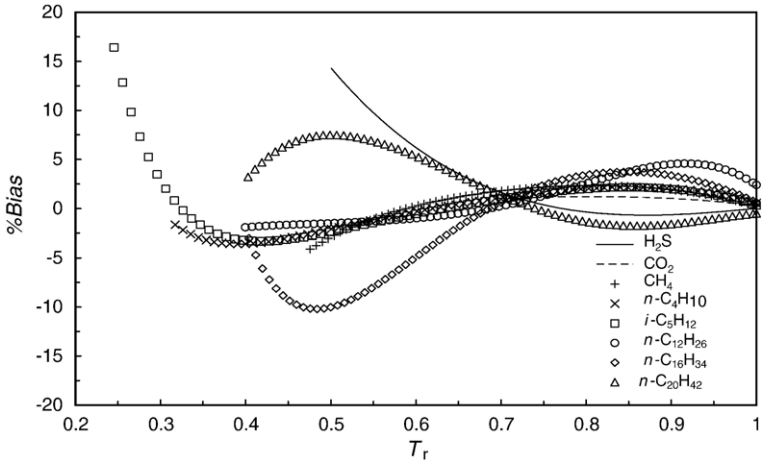

Fig. 1. Percent bias between experimental (Daubert and Danner, 1992) and predicted vapor pressure of some natural gas constituents from the triple point to the critical point. The predictions are from Eq. (6) and %Bias is defined by: %Bias=(100)(cald−exp *l*)/exp *l*.

subcritical and supercritical behavior of fluids not only attributes to the pressure–volume–temperature (*PVT*) relationship of the EoS but also to the temperature dependency of the α function. A general two constant EoS may be defined by (Michelsen and Mollerup, 2004):

$$P = \frac{RT}{v-b} - \frac{a_C \alpha(T_r)}{(v+\delta_1 b)(v+\delta_2 b)} \tag{1}$$

with

$$b = \Omega_b \frac{RT_C}{P_C} \tag{2}$$

$$a_C = \Omega_a \frac{R^2 T_C^2}{P_C} \tag{3}$$

where P is the pressure, T is the temperature, v is the specific volume, R is the gas constant, b is the molar covolume, a is the attractive parameter, and Ω_b and Ω_a are two coefficients which depend on the constants δ_1 and δ_2. The subscripts r and C stand for the reduced and critical properties. At the critical temperature, the second viral coefficient of Eq. (1) is expressed by:

$$\frac{B_{2,C} P_C}{RT_C} = \Omega_b - \Omega_a \tag{4}$$

where $B_{2,C}$ is the second virial coefficient at the critical temperature. Mathias (2003) pointed out that the reduced second virial coefficient ($B_{2,C}P_C/RT_C$) of most fluids at the critical point is nearly −0.34. When this condition is applied to Eq. (4), one can obtain:

$$\Omega_b - \Omega_a \approx -0.34 \tag{5}$$

Eq. (5) would be the constraint for obtaining the EoS of natural gas mixtures.

Nasrifar and Bolland (2004) improved Soave's α function on the basis of the equality of the second virial coefficient from the RKS EoS and the square-well potential. The obtained α function, in general, improves the accuracy of the RKS EoS in predicting the pure component compressibility factor and fugacity at supercritical temperatures. Accurate fugacity of pure compounds is particularly important, as shown by Flöter et al. (1998), in calculating the fluid phase equilibria of asymmetric hydrocarbon mixtures containing methane. However, the fugacity of fluids for an EoS is usually

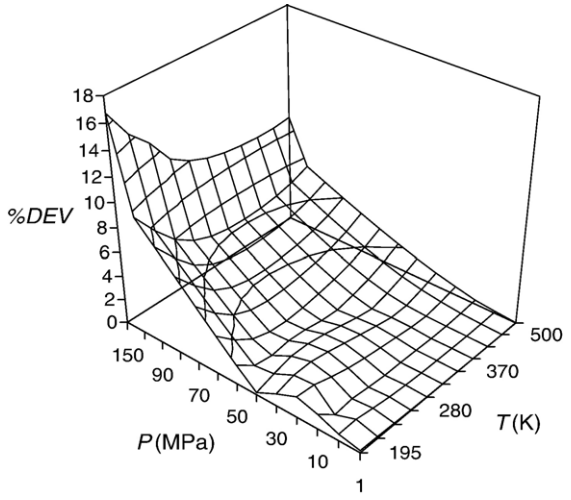

Fig. 2. Percent absolute deviations between the IUPAC-recommended values (Wagner and de Reuck, 1996) and predicted fugacities of methane as functions of temperature and pressure. The predictions are from Eq. (6) and %Dev is defined by: %Dev=(100)|cald−exp *l*|/exp *l*.

fixed indirectly by correlating the EoS to the vapor pressure of pure compounds along the coexistence curve. It is also worth noting that all two-constant EoSs similar in form to Eq. (1) have a fixed value of fugacity at the critical point. The critical fugacity coefficient of the RKS EoS is equal to 0.6657 and 0.6457 for the PR EoS (Michelsen and Mollerup, 2004). The reported value for the fugacity coefficient of methane at the critical point (Younglove and Ely, 1987) is 0.6640, however. If Eq. (1) is to be used to predict the thermodynamic properties of methane (natural gas) in supercritical region, the starting point which is the critical point, should also be predicted accurately. It should be noted that the accuracy of EoSs in engineering is based on the adequacy of the critical point to predict the subcritical and supercritical properties. As such, it is essential for the EoS of natural gas systems to predict the critical fugacity of methane (as the major component) accurately. However, it is worth stressing that the accurate prediction of fugacity of methane by the EoS of natural gas system is only a necessary condition. On the basis of this premise and Eq. (5) as the constraint, we concluded that $\delta_1=\delta_2=1/\sqrt{3}$ would meet these requirements. Incorporating these values in Eq. (1), a new *PVT* relationship is obtained:

$$P=\frac{RT}{v-b}-\frac{a_C\alpha(T_r)}{\left(v+b/\sqrt{3}\right)^2} \tag{6}$$

with

$$b=0.079246\frac{RT_C}{P_C} \tag{7}$$

$$a_C=0.421875\frac{R^2T_C^2}{P_C} \tag{8}$$

At the critical point, the compressibility factor, second virial coefficient, and fugacity coefficient of Eq. (6) were found to be 0.329, −0.342, and 0.6640, respectively.

For the α function, the modified Soave's α function by Nasrifar and Bolland (2004) is used:

$$\alpha(T_r)=\begin{cases}\left[1+m\left(1-\sqrt{T_r}\right)\right]^2 & T_r\le 1\\ \dfrac{b_1}{T_r}+\dfrac{b_2}{T_r^2}+\dfrac{b_3}{T_r^3} & T_r>1\end{cases} \tag{9}$$

with

$$b_1=0.25(12-11m+m^2) \tag{10}$$

$$b_2=0.5(-6+9m-m^2) \tag{11}$$

$$b_3=0.25(4-7m+m^2) \tag{12}$$

where the parameter m was determined by correlating the vapor pressure of pure substances from the triple point to the critical point temperature. These obtained parameters were correlated in terms of acentric factor (ω). The final correlation is expressed by:

$$m=0.4857+1.6308\omega-0.2089\omega^2 \tag{13}$$

where ω ranges from −0.216 to 0.8764.

3. Extension to mixtures

The classical van der Waals mixing rules were used to extend Eq. (6) to mixtures:

$$b=\sum_j x_jb_j \tag{14}$$

$$a=\sum_i\sum_j x_ix_ja_{ij} \tag{15}$$

with

$$a_{ij}=\sqrt{a_ia_j}(1-k_{ij}) \tag{16}$$

where x is the liquid/vapor mole fraction and k_{ij} is the binary interaction parameter. In this work, $k_{ij}=0$, otherwise it is stated.

4. Results and discussion

A natural gas mixture is a system different from the pure components. Thence, the properties of natural gas mixtures are quite dependent on composition. Nevertheless, if the EoS is accurate at representing pure component properties as limiting cases, the EoS must also be accurate at representing natural gas properties.

Table 2
Accuracy of the EoSs in predicting the fugacity of methane for wide ranges of temperature and pressure

EOS	%AAD[a]
This work	2.29
RKS	3.56
RKSNB	2.55
RKTCC	5.29
PR	8.37
PRGGPR	7.70
MNM	8.18
3M	3.76
HY	2.00
BWRS	7.02

[a] Experimental data from Wagner and de Reuck (1996); number of points=142; $195\le T(K)\le 600$ and $1\le P(MPa)\le 150$.

Table 3
Liquefied natural gas mixture compositions and code names (experimental data from Haynes and Hiza, 1977; Hiza and Haynes, 1980; Haynes, 1982)

Code	N_2	C_1	C_2	C_3	i-C_4	n-C_4	i-C_5	n-C_5
LNG1		0.8604, 0.85378	0.0460, 0.05178	0.0479, 0.0470	0.0457, 0.04741			
LNG2	0.04801	0.8094	0.04542	0.0505	0.04667			
LNG3		0.8534, 0.75442	0.07895, 0.15401	0.04729, 0.06950	0.00854, 0.00978	0.00992, 0.00978	0.00097, 0.00089	0.00089, 0.00083
LNG4	0.0484	0.8526	0.0483	0.0507				
LNG5		0.84558–0.85892	0.05042–0.11532	0.4038–0.01341	0.0053–0.02577	0.00705–0.02901		
LNG6	0.049	0.8060	0.0468	0.0482	0.050			
LNG7	0.0554	0.7909	0.056	0.0500		0.0477		
LNG8	0.00601–0.0425	0.8130–0.90613	0.0475–0.08477	0.02154–0.0298	0.00300–0.0241	0.00306–0.0242		
LNG9		0.85133, 0.84566	0.05759, 0.07924	0.04808, 0.05060		0.02450, 0.04300		
LNG10	0.00599–0.00859	0.74275–0.90068	0.06537–0.16505	0.02200–0.06742	0.00291–0.01336	0.00284–0.01326	0.00010–0.00223	0.00011–0.00216
LNG11		0.85341	0.07898	0.04729	0.00854	0.00992	0.00097	0.00089
LNG12		0.86040	0.04600	0.04790	0.0457			
LNG13	0.0484	0.8094	0.04542	0.05050	0.04628			
LNG14	0.0484	0.8526	0.0453	0.0537				
LNG15		0.85443	0.05042	0.04038	0.02577	0.02900		
LNG16	0.049	0.8060	0.0468	0.0482	0.0500			
LNG17	0.0554	0.7909	0.056	0.05		0.0477		
LNG18	0.0425	0.8130	0.0475	0.0487	0.0241	0.0242		
LNG19		0.85133	0.05759	0.04808		0.0430		
LNG20	0.00599	0.74275	0.16505	0.06547	0.00843	0.00893	0.00069	0.00269

Table 1 presents the accuracy of Eq. (6) in predicting the vapor pressure of common components in natural gas mixtures from the triple point to the critical point. Given in Table 1 are also predictions from the PR EoS, modified PR EoS by Gasem et al. (2001) (PRGGPR), the RKS EoS, modified Redlich

Table 4
Accuracy (%AAD) of the EoSs in predicting the saturated liquid density of the LNG mixtures

Code	T range (K)	n	This work	RKS/RKSNB	RKTCC	PR	PRGGPR	MNM	3M
LNG1	115–135	9	4.30	1.98	1.96	10.55	10.74	0.81	0.82
LNG2	115–130	4	4.59	1.70	1.68	10.86	11.06	0.50	0.57
LNG3	110–130	9	4.61	1.89	1.90	10.56	10.75	1.43	1.31
LNG4	105–120	4	5.58	0.84	0.91	11.80	11.97	1.31	0.94
LNG5	105–130	12	4.63	1.75	1.77	10.76	10.94	1.32	1.06
LNG6	105–120	4	4.99	1.64	1.62	10.78	10.99	1.27	1.73
LNG7	105–130	6	4.82	1.67	1.65	10.82	11.02	0.94	0.97
LNG8	115–130	9	4.34	1.95	1.93	10.58	10.77	0.82	0.53
LNG9	105–130	15	4.80	1.45	1.48	11.17	11.34	1.05	0.72
LNG10	110–130	13	4.54	1.90	1.91	10.58	10.76	1.30	1.22
LNG11	110–130	5	4.69	1.67	1.69	10.81	11.05	1.21	0.88
LNG12	115–135	5	4.23	1.99	1.98	10.55	10.74	0.75	0.74
LNG13	115–130	4	4.59	1.70	1.68	10.86	11.06	0.50	0.57
LNG14	105–120	4	5.58	0.84	0.91	11.80	11.97	1.31	0.94
LNG15	105–120	4	4.61	2.05	2.02	10.30	10.51	1.94	1.96
LNG16	105–120	4	4.99	1.64	1.62	10.78	10.99	1.27	1.73
LNG17	105–110	2	5.17	1.65	1.61	10.69	10.92	1.56	1.93
LNG18	105–120	4	4.91	1.73	1.69	10.68	10.90	1.33	1.56
LNG19	115–135	5	4.20	2.06	2.02	10.46	10.65	0.71	0.48
LNG20	110–125	4	4.33	2.33	2.33	9.99	10.18	1.84	1.98
Overall		126	4.66	1.74	1.74	10.76	10.95	1.16	1.13

Table 5
Natural gas mixture compositions and code names for calculating compressibility factors and speeds of sound data

Component	M1 [a, b]	M2 [a, b]	M3 [a, b]	M4 [a, b]	M5 [a, b]	M6 [c]	M7 [c]	M8 [c]	M9 [d]	M10 [d]	M11 [e]	M12 [e]	M13 [e]	M14 [e]
He							0.00015							
O_2							0.00011							
N_2	0.00269	0.03134	0.13575	0.05703	0.01007	0.00841	0.01474	0.05751		0.09922	0.00262	0.03113	0.00718	0.00537
CO_2	0.00589	0.00466	0.00994	0.07592	0.01498	0.00066	0.00647	0.00052		0.02000	0.00597	0.00500	0.00756	0.01028
C_1	0.96580	0.90644	0.81299	0.81203	0.85898	0.98352	0.90362	0.92436	0.84902	0.80051	0.96561	0.90708	0.83980	0.74348
C_2	0.01815	0.04553	0.03294	0.04306	0.08499	0.00511	0.05708	0.01285	0.15098	0.05023	0.01829	0.04491	0.13475	0.12005
C_3	0.00405	0.00833	0.00637	0.00894	0.02296	0.00153	0.01124	0.00348		0.03004	0.00410	0.00815	0.00943	0.08251
i-C_4	0.00099	0.00100	0.00101	0.00148	0.00351	0.00021	0.00301	0.00041			0.00098	0.00106	0.00040	
n-C_4	0.00102	0.00156	0.00100	0.00155	0.00347	0.00031	0.00169	0.00046			0.00098	0.00141	0.00067	0.03026
i-C_5	0.00047	0.00030			0.00051	0.00008	0.00059	0.00015			0.00046	0.00027	0.00013	
n-C_5	0.00032	0.00045			0.00053	0.00011	0.00029	0.00014			0.00032	0.00065	0.00008	0.00575
n-C_6	0.00063	0.00040				0.00005	0.00058	0.00012			0.00067	0.00034		
n-C_7						0.00001	0.00035							
n-C_8						0.000003	0.00008							

[a] Magee et al. (1997).
[b] Hwang et al. (1997).
[c] Čapla et al. (2002).
[d] Costa Gomes and Trusler (1998).
[e] Younglove et al. (1993).

Table 6
Accuracy (%AAD) of the EoSs in predicting the compressibility factor of natural gas mixtures

Code	n	T range (K)	P range (MPa)	This work	RKSNB	RKS	RKTCC	PR	PRGGPR	MNM	3M	BWRS	HY
M1	143	225–350	0.19–34.27	0.52	1.25	1.37	2.15	1.68	1.53	2.59	1.47	0.85	0.44
M2	144	225–350	0.20–34.50	0.44	1.16	1.31	2.07	1.76	1.60	2.66	1.37	0.81	0.52
M3	144	225–350	0.18–34.65	0.30	0.84	1.07	1.67	1.86	1.70	2.63	1.06	0.79	0.70
M4	168	225–350	0.19–33.13	0.47	0.71	0.82	1.36	2.48	2.32	3.52	0.78	0.76	1.42
M5	125	250–350	0.19–32.95	0.53	1.31	1.46	2.32	1.97	1.81	2.92	1.40	0.83	0.45
M6	28	253–323	0.99–15.00	0.70	1.50	1.67	2.72	1.89	1.70	3.12	2.17	0.85	0.99
M7	28	253–323	1.00–15.02	0.66	1.53	1.72	2.87	2.09	2.60	3.48	2.13	0.87	0.44
M8	28	253–323	1.00–15.00	0.54	1.32	1.56	2.52	1.96	1.76	3.13	1.98	0.77	1.17
Average	808			0.47	1.08	1.23	1.97	1.97	1.83	2.92	1.29	0.81	0.75

and Kwong (1949) EoS by Twu et al. (1995) (RKTCC), modified RKS EoS by Nasrifar and Bolland (2004) (RKSNB), modified Nasrifar and Moshfeghian (2004) (MNM), and Mohsen-Nia et al. (1994) (3M) EoS. In 2001, Gasem et al. (2001) modified the temperature dependency of the PR EoS in order to improve the PR EoS in predicting vapor pressure and eliminating the anomalous behavior of the PR's α function at elevated temperatures. The impetus for modifying the RK EoS by Twu et al. (1995) had been the same as the impetus for modifying the PR EoS by Gasem et al. (2001). However, Nasrifar and Bolland (2004) attempted to augment the supercritical behavior of the RKS EoS using the square-well potential. The MNM and 3M EoS are two cubic EoSs with temperature dependent molecular co-volume parameter. As a result, these two are expected to accurately predict the liquid density of hydrocarbons. With exception of the PR, MNM and 3M EoSs, the other EoSs predict the vapor pressure of pure substances with similar accuracy. In this work, accuracy is defined in terms of average of absolute deviations (%AAD). The %AAD may be expressed by:

$$\%\mathrm{AAD} = (100/n)\sum_j |\mathrm{cald}_j - \exp l_j|/\exp l_j \qquad (17)$$

In predicting vapor pressure of natural gas constituents, the %AAD was found to be 8.14% for the PR EoS, 5.24% for the MNM EoS, 9.06% for 3M and about 3% for the rest.

Fig. 1 shows a deviation plot for predicting the vapor pressure of some components in natural gas mixtures using Eq. (6). Clearly, deviations propagate around zero with reasonable accuracy except for H_2S and i-C_5H_{12} at low reduced temperatures.

As mentioned before, the supercritical behavior of methane must be effective on the thermodynamic properties of natural gas mixtures. A property that can reflect the accuracy of Eq. (6) in predicting the supercritical behavior of methane is fugacity. Fig. 2 displays the percent absolute deviation in predicting the fugacity of methane by use of Eq. (6). The temperature ranges from 195 K to 500 K and pressure from 1 MPa to 150 MPa. The deviations are larger at low temperatures and increases with pressure. However, up to 90 MPa, the deviations are remarkably small no matter what the temperature is. The %AAD was found to be 2.29% for Eq. (6). For the EoSs mentioned above, modified BWR EoS by Starling (1973) (BWRS) and a quite accurate EoS for the compressibility factor of natural gas mixtures by Hall and Yarborough (1973), the results are given in Table 2. As can be seen in Table 2, the HY EoS is absolutely superior. The next best EoSs are, respectively, Eq. (6) and the RKSNB EoS. This high accuracy attributes to the use of Eq. (9) as the α function for both EoSs.

Table 7
Accuracy (%AAD) of the EoSs in predicting the speeds of sound for natural gas mixtures

Code	n	T range (K)	P range (MPa)	This work	RKSNB	RKS	RKTCC	PR	PRGGPR	MNM	3M	BWRS	HY
M9	36	250–350	0.50–20	1.69	1.71	2.12	2.29	2.24	1.98	1.61	2.45	2.33	2.24
M10	35	250–350	0.50–20	1.04	1.11	1.77	1.70	1.66	1.34	1.33	1.92	2.29	1.08
M11	83	250–350	0.50–10.71	0.46	0.90	1.31	1.62	1.03	0.83	1.73	2.39	0.76	0.57
M12	82	250–350	0.65–10.88	0.47	0.74	1.11	1.32	1.09	0.87	1.62	2.00	0.86	0.64
M13	91	250–350	0.50–10.40	0.68	1.19	1.54	1.70	1.11	0.98	1.74	2.35	0.89	0.63
M14	44	300–350	0.42–10.40	0.56	1.25	1.77	1.96	1.00	0.82	1.64	1.88	0.87	0.34
Overall	371			0.70	1.08	1.50	1.69	1.24	1.03	1.65	2.19	1.12	0.78

Table 8
Natural gas mixtures compositions and code names for calculating isobaric heat capacity, Joule–Thomson coefficient and VLE calculations

Component	M15 [a]	M16 [a]	M17 [b]	M18 [b]	M19 [c]	M20 [d]	M21 [e]	M22 [f]	M23 [g]
N_2		0.09939	0.03187	0.00496	0.0048		0.0008	0.0048	0.05651
CO_2		0.02090	0.01490		0.0015		0.0244		0.00284
C_1	0.84874	0.79942	0.88405	0.89569	0.8064	0.9135	0.8210	0.887634	0.833482
C_2	0.15126	0.05029	0.05166	0.08348	0.0593	0.0403	0.0578	0.0854	0.07526
C_3		0.03000	0.01176	0.01197	0.0298	0.0153	0.0287	0.0168	0.02009
i-C_4			0.00149	0.00149			0.0056	0.0022	0.00305
n-C_4			0.00226	0.00226		0.0082	0.0123	0.0029	0.0052
i-C_5			0.00056	0.00015			0.0052	0.000182	0.0012
n-C_5			0.00049		0.0430	0.0034	0.0060	0.000084	0.00144
i-C_6			0.000216						
n-C_6			0.000136			0.0039	0.0072		0.00068
C_6H_6			0.000272						
cyc-C_6			0.000065						
i-C_7			0.00010						
n-C_7			0.000041		0.0308				0.000138
CH_3-*cyc*-C_6			0.000052						
$C_6H_5CH_3$			0.000030						
i-C_8			0.000029						
n-C_8			0.000008						0.00011
i-C_9			0.000009						
n-C_9			0.000002						
n-C_{10}					0.0244				
C_{7+}						1.54 [h]	3.10 [i]		

[a] Ernst et al. (2001).
[b] Barreau et al. (1996).
[c] Yarborough and Vogel (1967).
[d] Hoffmann et al. (1953).
[e] Firoozabadi et al. (1978).
[f] Avila et al. (2002a).
[g] Avila et al. (2002b).
[h] C_{7+} specification: SG (60/60)=0.7961, MW=138.78.
[i] C_{7+} specification: SG (60/60)=0.7740, MW=132.

Table 3 gives the composition and code names for 20 LNG mixtures. On the basis of the components in mixtures, the LNG mixtures were coded. As indicated in Table 3, some mixtures have two or more compositions but the same components. The saturated liquid density of these LNG mixtures were predicted by Eq. (6) and compared with experimental data in Table 4. Also given in Table 4 are the predictions from the other EoSs. It is worth considering that the RKS and RKSNB EoSs predict the saturated liquid density of LNG mixtures with the same accuracy. In fact, at conditions where these LNG mixtures were studied, methane is subcritical and nitrogen is slightly supercritical. In other words, the RKSNB EoS reduces to the RKS EoS and hence both have the same accuracy. Clearly, the 3M and MNM EoSs predict the saturated liquid density of LNG mixtures with best accuracy. The %AAD was found to be around 1.15% for both EoSs. This high accuracy is attributed to the temperature dependency of the molecular co-volume in both EoSs. The RKS, RKSNB and RKTCC EoSs predict the saturated liquid densities with an average %AAD of 1.74%. The average

Table 9
Accuracy (%AAD) of the EoSs in predicting the isobaric heat capacity of natural gas mixtures

Code	*n*	*T* range (K)	*P* range (MPa)	This work	RKSNB	RKS	RKTCC	PR	PRGGPR	MNM	3M	BWRS	HY
M15	56	250–350	0.6–30	1.50	1.61	1.49	2.20	1.90	1.90	3.23	2.21	2.41	5.61
M16	54	250–350	0.6–30	0.95	1.02	0.98	1.41	1.55	1.54	3.15	1.16	1.99	7.03
M17	30	308–406	15–40	1.13	1.16	0.96	2.52	0.80	0.73	3.64	21.56	1.81	9.67
M18	30	308–406	15–40	2.30	2.34	2.07	3.87	0.99	1.04	2.56	0.94	2.97	8.06
Overall	170			1.40	1.47	1.34	2.30	1.43	1.43	3.16	5.07	2.27	7.21

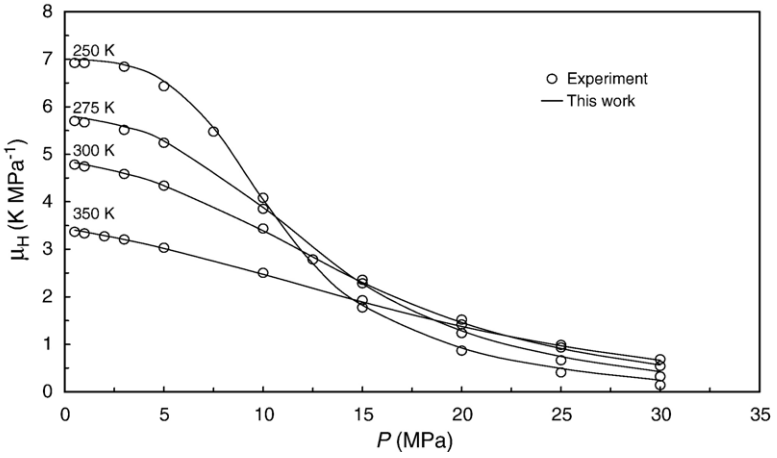

Fig. 3. Experimental (Ernst et al., 2001) and predicted Joule–Thomson coefficients for the natural gas mixture M16.

%AAD for Eq. (6) is 4.66% and 10.76% and 10.95% for the PR and PRGGPR EoSs, respectively. Table 4 also indicates that the accuracy of an EoS in predicting the liquid density of LNG mixtures is a consequence of the *PVT* relationship and nearly independent of the α function. Further, Table 4 indicates that the accuracy of Eq. (6) in predicting the saturated liquid densities of LNG mixtures lies between the RK family and PR family EoSs.

Table 5 presents the compositions and code names for 14 natural gas mixtures used for predicting the compressibility factor and speeds of sound data. In Tables 6 and 7, the accuracy of the EoSs is compared for predicting the compressibility factors and speeds of sounds data, respectively. Clearly, with exception of the HY EoS, Eq. (6) is remarkably superior with respect to the other EoSs for predicting these two properties. The average %AAD was found to be 0.47% for predicting the compressibility factors and 0.70% for the speeds of sound. For predicting these two properties, however, the HY EoS is only a little inferior with respect to Eq. (6).

Table 10
Accuracy of the EoSs in predicting Joule–Thomson coefficients for the mixture M16

EOS	%AAD[a]
This work	5.03
RKS	5.10
RKSNB	4.50
RKTCC	6.74
PR	12.03
PRGGPR	13.11
MNM	9.14
3M	9.31
HY	8.34
BWRS	9.89

When the RKS and RKSNB EoSs are compared, it is seen that the use of Eq. (9) as the modified Soave's α function improves the accuracy of the RKS EoS in predicting these two properties of natural gas mixtures.

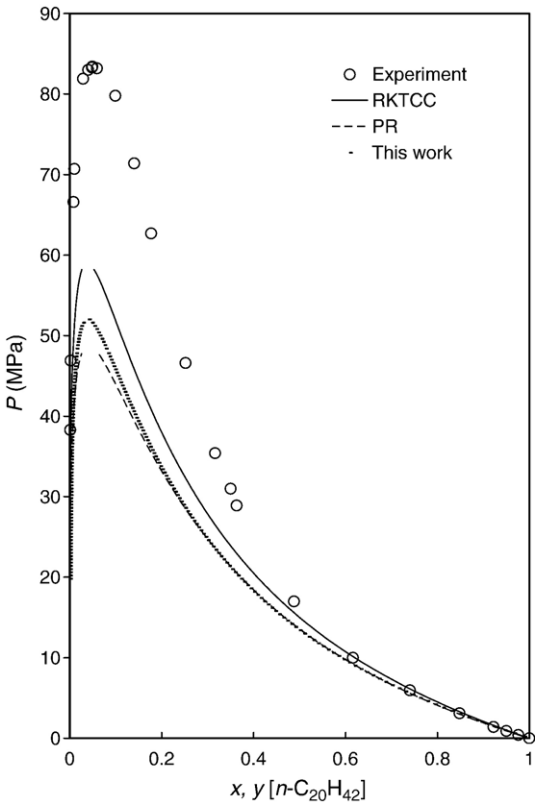

Fig. 4. Experimental (Van der Kooi et al., 1995) and predicted phase equilibria for the natural gas model mixture CH_4+n-$C_{20}H_{42}$ at 323.15K.

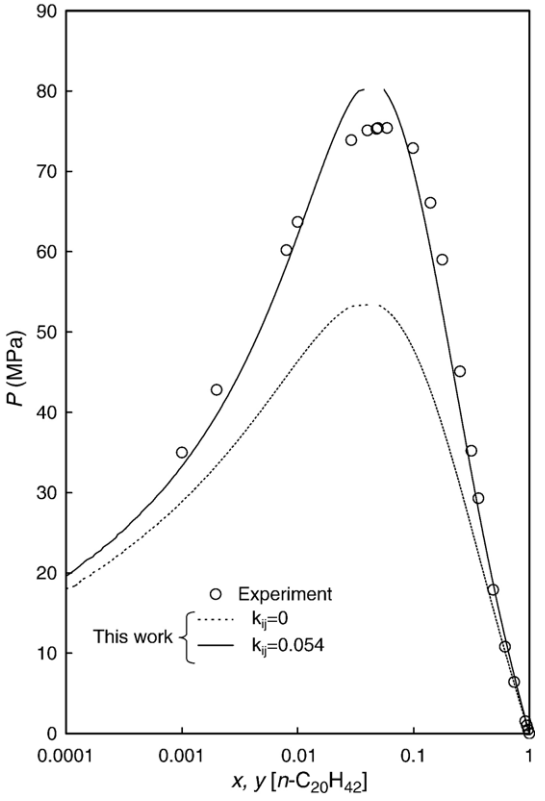

Fig. 5. Experimental (Van der Kooi et al., 1995), predicted and correlated phase equilibria for the natural gas model mixture CH_4+*n*-$C_{20}H_{42}$ at 353.15 K.

Table 8 gives the compositions and code names for 9 other natural gas mixtures. These mixtures are used in calculating isobaric heat capacity, Joule–Thomson coefficient and vapor–liquid–equilibria (VLE) of natural gas mixtures. In Table 9, the accuracy of Eq. (6) in predicting the isobaric heat capacity of 4 natural gas mixtures is presented. The RKTCC and BWRS EoSs predict the isobaric heat capacity of the natural gas mixtures with an average %AAD of 2.3%, the HY EoS with 7.2%, the MNM EoS with 3.16%, the 3M EoS with 5.07% and the rest with an average %AAD of about 1.40%. However, the RKS EoS with a %AAD of 1.34%, is slightly superior among the others. Eq. (6) is ranked number 2 in this comparison.

Fig. 3 shows Joule–Thomson coefficient for the natural gas mixture M16 as functions of pressure and temperature. As can be seen, the agreement with experimental data is quite good. The %AAD was found to be 5.03%. The same calculations were performed by the other EoSs with the %AAD given in Table 10. The RKSNB EoS with a %AAD of 4.5% is the best among the others. Eq. (6) is the second among the others.

Fig. 4 depicts experimental and predicted bubble and dew points for a model system comprised of methane and *n*-eicosane at 323.15 K. Among the EoSs used in this study, the RKTCC EoS predicts the experimental values more accurately than the others while the PR EoS predicts with the worst accuracy. The other EoSs including Eq. (6) lie between these two extremes. For clarity, only the predictions from Eq. (6) are illustrated. Nevertheless, because of large non-ideality for these asymmetric mixtures, none of the EoSs is predictive enough to agree with the experimental data. However, the *VLE* of binary asymmetric mixtures can easily be correlated using a single binary interaction parameter, as shown in Fig. 5, for the same system at 353.15 K. As such, a paper by Jaubert and Mutelet (2004) is particularly useful where the authors predicted/correlated the binary interaction parameters of a wide variety of systems using a group contribution method with the PR EoS.

The accurate prediction of equilibrium ratios for components in a gas mixture is of primary concerns in *VLE* calculations. Fig. 6 shows equilibrium ratios of the natural gas mixture M19 as a function of pressure at

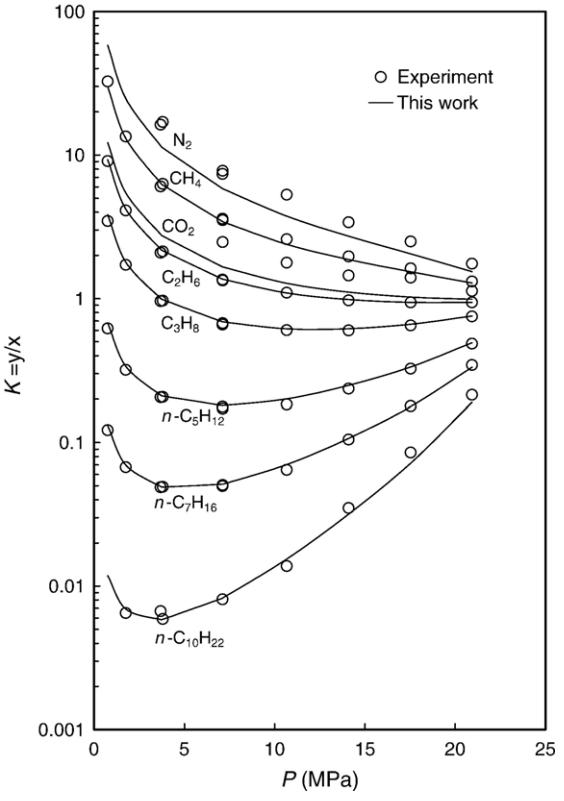

Fig. 6. Experimental (Yarborough and Vogel, 1967) and predicted equilibrium ratios for the natural gas mixture M19.

Table 11
Experimental (Hoffmann et al., 1953) and predicted dew points for the gas condensate mixture M20

Component	Vapor (mol%)	Liquid (mol%)							
		Experimental	This work	RKSNB	RKS	RKTCC	PR	PRGGPR	MNM
C_1	91.35	52.00	63.326	62.798	62.510	62.010	60.153	60.104	49.264
C_2	4.03	3.81	4.454	4.454	4.485	4.521	4.401	4.420	3.605
C_3	1.53	2.37	2.315	2.326	2.346	2.380	2.347	2.3440	1.893
n-C_4	0.82	1.72	1.698	1.711	1.726	1.756	1.758	1.7420	1.409
n-C_5	0.34	1.20	0.936	0.946	0.954	0.969	0.987	0.9720	0.780
n-C_6	0.39	2.06	1.409	1.420	1.439	1.456	1.510	1.4760	1.180
C_{7+}	1.54	36.84	25.862	26.345	26.54	26.908	28.844	28.942	41.865
Dew point pressure (MPa)		26.46	28.806	28.867	29.63	31.251	26.808	28.13	35.48

366.44 K. As can be seen, the agreement between the predictions by Eq. (6) and experimental data is quite good except for nitrogen and carbon dioxide. Unless the compositions of these components are large, this inaccuracy will not pose problem. However, the inaccuracy might be alleviated by use of binary interaction parameters with mixing rules.

In Table 11, experimental and predicted dew point pressures and liquid compositions for the gas condensate mixture M20 are compared. In order to perform calculations, the C_{7+} fraction was split into 12 single carbon number groups (SCN) using the logarithm distribution described by Pedersen et al. (1992). The critical properties and acentric factor of each group were determined by Twu's correlations (Twu, 1984). After characterizing the C_{7+} fraction, the *VLE* calculations were performed. The results are given in Table 11. Comparison with experimental data indicates that PR EoS accurately predicts the natural gas mixture dew point at 367 K. The RKSNB, PRGGPR and Eq. (6) are the next best EoSs in agreement with the experimental value while the MNM EoS is the worst among the others. Nevertheless, only the MNM EoS predicts the liquid phase compositions rather accurately.

Table 12 gives flash yields for the gas condensate mixture M21. The heavy fraction was characterized similarly to the gas condensate mixture M20. With exception of the MNM EoS, the predictions are similar in accuracy. However, the MNM EoS is slightly more accurate.

Fig. 7 shows phase envelope for the natural gas mixture M22. In addition to Eq. (6), the RKTCC, RKSNB and PRGGPR EoSs were used to predict the phase envelope. The phase envelope predicted by the PRGGPR is clearly the least accurate among the others while Eq. (6), the RKTCC and RKSNB EoSs are similar in accuracy. Also, in a previous work, Nasrifar et al. (2005) reached to a similar conclusion. Fig. 8 shows the phase envelope for the natural gas mixture M23. The experimental values are from Avila et al. (2002b) and predicted values from Eq. (6), and three other EoSs: Schmidt and Wenzel (1980) (SW), modified Patel and Teja (1982) by Valderrama (1990) (PTV) and Guo and Du (1989) (GD). The SW EoS and Eq. (6) are clearly in better agreement with experimental data when compared to the other EoSs. While Eq. (6) slightly underestimates the experimental data, the SW EoS overestimates. The PTV and GD EoSs predictions lie inside the experimental phase envelope.

5. Conclusions

A two-constant cubic EoS has been introduced by matching the critical fugacity coefficient of the EoS equal to the fugacity coefficient of methane at the critical point. A recently augmented Soave's α function

Table 12
Experimental (Firoozabadi et al., 1978) and predicted flash yields for the retrograde condensation of mixture M21

T (K)	P (MPa)	L/F [a]							
		Experimental	This work	RKSNB	RKS	RKTCC	PR	PRGGPR	MNM
278.15	14.6	0.1106	0.1727	0.1712	0.1703	0.1608	0.1694	0.1649	0.1174
278.15	20.8	0.0993	0.1077	0.1122	0.1152	0.1276	0.0915	0.1025	0.0692
318.15	14.6	0.0659	0.1010	0.0997	0.0988	0.0956	0.0946	0.0931	0.0739
318.15	20.8	0.0333	0.0857	0.0853	0.0862	0.0877	0.0746	0.0754	0.0532

[a] L/F is the liquid to feed molar ratio.

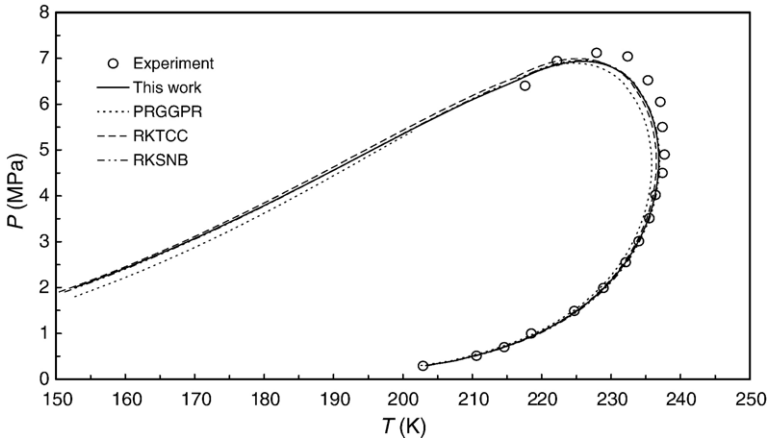

Fig. 7. Experimental (Avila et al., 2002a) and predicted phase envelopes for the natural gas mixture M22.

has been used for the temperature dependence of the attractive parameter in the EoS. The developed EoS has predicted the natural gas compressibility factors and speeds of sound data of some natural gas mixtures better than the expected accuracy of two-constant EoSs. In predicting these properties, the new EoS has shown remarkable superiority when compared to other EoSs, especially the cubic ones. The accuracy of the EoS in predicting other natural gas properties, i.e., isobaric heat capacity, Joule–Thomson coefficient, and calculating dew points, phase envelopes and flash yields, is similar to the RK family EoSs.

List of symbols

a	attractive parameter
b	molar co-volume
b_1, b_2, b_3	parameters defined by Eqs. (10)–(12)
B_2	second virial coefficient
k_{ij}	binary interaction parameter
m	parameter defined by Eq. (13)
n	number of points
P	pressure
R	universal gas constant
T	temperature
v	volume
x	mole fraction

Acronyms

3M	Mohsen–Nia–Moddaress–Mansoori
BWRS	Benedict–Webb–Rubin–Starling
EoS	Equation of state
GD	Guo–Du
HY	Hall–Yarborough
MNM	Modified–Nasrifar–Moshfeghian
PR	Peng–Robinson
PRGGPR	Peng–Robinson–Gasem–Gao–Pan–Robinson
PTV	Patel–Teja–Valderrama

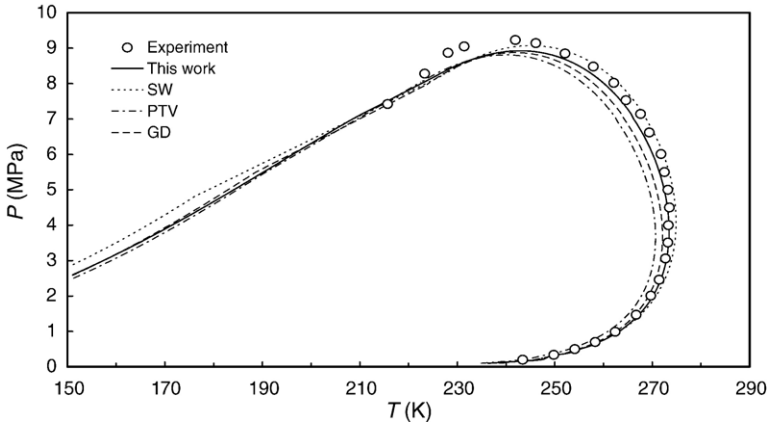

Fig. 8. Experimental (Avila et al., 2002b) and predicted phase envelopes for the natural gas mixture M23.

RK Redlich–Kwong
RKS Redlich–Kwong–Soave
RKSNB Redlich–Kwong–Soave–Nasrifar–Bolland
RKTCC Redlich–Kwong–Twu–Coon–Cunningham
SW Schmidt–Wenzel

Greek Letters

α temperature dependence for attractive parameter
δ_1, δ_2 constants in Eq. (1)
ω acentric factor
Ω_a, Ω_b constants in Eqs. (2) and (3)

Subscripts

c critical property
r reduced property

Acknowledgement

The authors express their appreciations to Statoil, Norway, for supporting this work.

References

AGA, Report No. 3= ANSI/API 2530, 1978. Orifice Metering of Natural Gas. American National Standard Institute (ANSI), New York.

Avila, S., Blanco, S.T., Velasco, I., Rauzy, E., Otín, S., 2002a. Thermodynamic properties of synthetic natural gases: 2. Dew point curves of synthetic natural gases and their mixtures with water and methanol. Measurement and correlation. Energy Fuels 16, 928–934.

Avila, S., Blanco, S.T., Velasco, I., Rauzy, E., Otín, S., 2002b. Thermodynamic properties of synthetic natural gases: 1. Dew-point curves of synthetic natural gases and their mixtures with water and methanol. Measurement and correlation. Ind. Eng. Chem. Res. 41, 3714–3721.

Barreau, A., Janneteau, P., Gaillard, K., 1996. Isobaric heat capacity of natural gases. Measurements and modelling. Fluid Phase Equilib. 119, 197–212.

Benedict, M., Webb, G.B., Rubin, L.C., 1940. An empirical equation for thermodynamic properties of light hydrocarbons and their mixtures, methane, ethane, propane and *n*-butane. J. Chem. Phys. 8, 334–345.

Čapla, L., Buryan, P., Jedelský, J., Rottner, M., Linek, J., 2002. Isothermal *PVT* measurements on gas hydrocarbon mixtures using a vibrating-tube apparatus. J. Chem. Thermodyn. 34, 657–667.

Costa Gomes, M.F., Trusler, J.P.M., 1998. The speed of sound in two methane-rich gas mixtures at temperatures between 250 K and 350 K and at pressures up to 20 MPa. J. Chem. Thermodyn. 30, 1121–1129.

Daubert, T.E., Danner, R.P., 1992. Physical and Thermodynamic Properties of Pure Chemicals, Data Compilation. Hemisphere Publishing Corp., London, UK.

Ernst, G., Keil, R., Wirbser, H., Jaeschke, M., 2001. Flow-calorimetric results for the massic heat capacity c_p and the Joule–Thomson coefficient of CH_4, of (0.85 CH_4+0.15 C_2H_6), and of a mixture similar to natural gas. J. Chem. Thermodyn. 33, 601–613.

Estela-Uribe, J.F., Trusler, J.P.E., 2001. Extended corresponding states equation of state for natural gas systems. Fluid Phase Equilib. 183–184, 21–29.

Estela-Uribe, J.F., De Mondoza, A., Trusler, J.P.E., 2004. Extended corresponding states model for fluids and fluid mixtures II. Application to mixtures and natural gas systems. Fluid Phase Equilib. 216, 59–84.

Firoozabadi, A., Hekim, Y., Katz, D.L., 1978. Reservoir depletion calculation for gas condensates. Can. Chem. Eng. 56, 610–615.

Flöter, E., de Loos, Th.W., de Swaan Arons, J., 1998. Improved modeling of the phase behavior of asymmetric hydrocarbon mixtures with the Peng–Robinson equation of state using a different temperature dependency of the parameter *a*. Ind. Eng. Chem. Res. 37, 1651–1662.

Gasem, K.A.M., Gao, W., Pan, Z., Robinson Jr., R.L., 2001. A modified temperature dependence for the Peng–Robinson equation of state. Fluid Phase Equilib. 181, 113–125.

Guo, T.-M., Du, L., 1989. A three-parameter cubic equation of state for reservoir fluids. Fluid Phase Equilib. 52, 47–57.

Hall, K.R., Yarborough, L., 1973. A new equation of state for *Z*-factor calculations. Oil Gas J. 18, 82–92 (June).

Haynes, W.M., 1982. Measurements of orthobaric-liquid densities of multicomponent mixtures of LNG components (N_2, CH_4, C_2H_6, C_3H_8, $CH_3CH(CH_3)CH_3$, C_4H_{10}, $CH_3CH(CH_3)C_2H_5$ and C_5H_{10}) between 110 and 130 K. J. Chem. Thermodyn. 14, 603–612.

Haynes, W.M., Hiza, M.J., 1977. Measurements of the orthobaric liquid densities of methane, ethane, propane, isobutane, and normal butane. J. Chem. Thermodyn. 9, 179–187.

Hiza, M.J., Haynes, W.M., 1980. Orthobaric liquid densities and excess volumes for multicomponent mixtures of low molar mass alkanes and nitrogen between 105 and 125 K. J. Chem. Thermodyn. 12, 1–10.

Hoffmann, A.E., Crump, J.S., Hocott, C.R., 1953. Equilibrium constants for a gas condensate system. Petrol. Trans. AIME 198, 1–10.

Hwang, C.-A., Simon, P.P., Hou, H., Hall, K.R., Holste, J.C., Marsh, K.N., 1997. Burnett and pycnometric (p, V_m, T) measurements for natural gas mixtures. J. Chem. Thermodyn. 29, 1455–1472.

Jaeschke, M., Audibert, S., van Caneghem, P., Humphreys, A.E., Janssen-van Rosmalen, R., Pellei, Q., Michels, J.P., Schouten, J.A., ten Seldam, C.A., 1989. High accuracy compressibility factor for natural gases and similar mixtures by use of a truncated virial equation. GERG Technical Monograph, vol. TM2.

Jaubert, J.-N., Mutelet, F., 2004. VLE prediction with Peng–Robinson equation of state and temperature dependent k_{ij} calculated through a group contribution method. Fluid Phase Equilib. 224, 285–304.

Magee, J.M., Haynes, W.M., Hiza, M.J., 1997. Isochoric (p, ρ, T) measurements for five natural Gas mixtures from T=(225 to 350) K at pressures to 35 MPa. J. Chem. Thermodyn. 29, 1439–1454.

Mathias, P.M., 2003. The second virial coefficient and the Redlich–Kwong equation. Ind. Eng. Chem. Res. 42, 7037–7044.

McCarty, R.D., 1982. Mathematical models for the prediction of liquefied-natural-gas densities. J. Chem. Thermodyn. 14, 837–854.

Michelsen, M.L., Mollerup, J.M., 2004. Thermodynamic models, fundamentals and computational aspects. Tie-Line Publication, Lyngby, Denmark.

Mohsen-Nia, M., Moddaress, H., Mansoori, G.A., 1994. Sour natural gas and liquid equation of state. J. Pet. Sci. Eng. 12, 127–136.

Nasrifar, Kh., Bolland, O., 2004. Square-well potential and a new α function for the Soave–Redlich–Kwong equation of state. Ind. Eng. Chem. Res. 43, 6901–6909.

Nasrifar, Kh., Moshfeghian, M., 2004. Application of an improved equation of state to reservoir fluids: computation of minimum miscibility pressure. J. Pet. Sci. Eng. 42, 223–234.

Nasrifar, Kh., Bolland, O., Moshfeghian, M., 2005. Predicting natural gas dew points from 15 equations of state. Energy Fuels 19, 561–572.

Patel, N.C., Teja, A.S., 1982. A new cubic equation of state for fluids and fluid mixtures. Chem. Eng. Sci. 37, 463–473.

Pedersen, K.S., Blilie, A.L., Meisingset, K.K., 1992. *PVT* calculations on petroleum reservoir fluids using measured and estimated compositional data for the plus fraction. Ind. Eng. Chem. Res. 31, 1378–1384.

Peng, D.-Y., Robinson, D.B., 1976. A new two-constant equation of state. Ind. Eng. Chem. Fundam. 15, 59–64.

Redlich, O., Kwong, J.N.S., 1949. On the thermodynamics of solutions: V. An equation of state: Fugacities of gaseous solutions. Chem. Rev. 44, 233–244.

Schmidt, G., Wenzel, H., 1980. A modified van der Waals type equation of state. Chem. Eng. Sci. 35, 1503–1512.

Soave, G., 1972. Equilibrium constants from a modified Redlich–Kwong equation of state. Chem. Eng. Sci. 27, 1197–1203.

Starling, K.E., 1973. Fluid Thermodynamic Properties for Light Petroleum Systems. Gulf Publishing Company, Texas, TX, pp. 220–221.

Twu, C.H., 1984. An internally consistent correlation for predicting the critical properties and molecular weights of petroleum and coal tar liquids. Fluid Phase Equilib. 16, 137–150.

Twu, C.H., Coon, J.E., Cunningham, J.R., 1995. A new generalized alpha function for a cubic equation of state: Part 2. Redlich–Kwong equation. Fluid Phase Equilib. 105, 61–69.

Valderrama, J.O., 1990. A generalized Patel–Teja equation of state for polar and nonpolar fluids and their mixtures. J. Chem. Eng. Jpn. 23, 87–91.

Van der Kooi, H.J., Flöter, E., de Loos, Th.W., 1995. High pressure phase equilibria of $\{(1-x)CH_4+xCH_3(CH_2)_{18}CH_3\}$. J. Chem. Thermodyn. 27, 847–861.

Wagner, W., de Reuck, K.M., 1996. (IUPAC). Methane. International Thermodynamic Tables of the Fluid State, vol. 13. Blackwell, Oxford, UK.

Yarborough, L., Vogel, J.L., 1967. A new system for obtaining vapor and liquid sample analyses to facilitate the study of multicomponent mixtures at elevated pressures. Chem. Eng. Symp. Ser. 63, 1–9.

Younglove, B.A., Ely, J.F., 1987. Thermophysical properties of fluids II. Methane, ethane, propane, isobutane, and normal butane. J. Phys. Chem. Ref. Data 16, 577–798.

Younglove, B.A., Frederick, N.V., McCarty, R.D., 1993. Speed of sound data and related models for mixtures of natural gas constituents. NIST Monograph, vol. 178.